Journal of Modern Optics, 2016
Vol. 63, No. 5, 495–500, http://dx.doi.org/10.1080/09500340.2014.922634

Taylor & Francis
Taylor & Francis Group

Improving the trapping capability using radially polarized narrow-width annular beam

Hua-Feng Xu[a,b], Wei-Jun Zhang[a,b], Jun Qu[c]* and Wei Huang[a,b]*

[a]*Laboratory of Atmospheric Physico-Chemistry, Anhui Institute of Optics & Fine Mechanics, Chinese Academy of Sciences, Hefei, China;* [b]*School of Environmental Science & Optoelectronic Technology, University of Science and Technology of China, Hefei, China;* [c]*Department of Physics, Anhui Normal University, Wuhu, China*

(*Received 26 February 2014; accepted 6 May 2014*)

A novel optical-trap method for improving the trapping capability using a radially polarized narrow-width annular beam (NWAB) has been proposed. In this paper, we theoretically study the tight focusing properties of a radially polarized NWAB, formed by subtly blocking the central portion of a radially polarized Bessel–Gaussian beam (the original doughnut beam), through a high-numerical aperture objective. It is shown that a sub-wavelength focal spot (0.32λ) with a quite long depth of focus (about 3λ) can be formed in the vicinity of the focus. Furthermore, the optical trapping forces acting on a metallic Rayleigh particle are calculated for the case where a radially polarized annular beam is applied. Numerical results show that the radially polarized NWAB can largely enhance the transverse trap stiffness and broaden the longitudinal trap range compared with the usage of the original doughnut beam. The influence of the annular factor δ on the focusing properties and the trap stiffness is investigated in detail.

Keywords: optical tweezers; optical trapping force; trap stiffness; radially polarized narrow-width annular beam

1. Introduction

Optical tweezers (originally called 'single-beam gradient force trap'), which are capable of trapping and manipulation small objects with non-contact forces by photon linear momentum transfer from light to matter, were derived from the seminal work of Ashkin et al. [1]. Since then, optical trapping and manipulation have been applied in various areas of science, particularly in physics, chemistry, and biophysical research, for example, trapping and cooling molecules and atoms [2], single aerosol trapping [3,4], trapping red blood cells in living animals [5], and so on. Thus, optical tweezers have been developed into a versatile and convenient tool in microscopic research [6].

Polarization, which describes the electric field oscillation direction of electromagnetic waves, is of particular interest. In recent years, cylindrical vector beams, such as radially and azimuthally polarized beams, have attracted extensive attention due to their unique focusing properties and potential applications, including optical data storage, material processing, and optical trapping [7–23]. A strong longitudinally polarized field component and a tighter spot beyond the diffraction limit can be created when a radially polarized beam is focused by a high-numerical aperture (NA) objective lens [10]. It is interesting that such a longitudinal field component can be efficiently suppressed or enhanced by amplitude [7,10,11], polarization [12] or phase modulation [13] of the incident beam. For example, using an annular aperture as an amplitude modulation device is an effective method to generate a sharper focal spot beyond the diffraction limit [7,11]. More recently, Yang et al. [11] have experimentally demonstrated the measurement of a tighter focal spot generated by a radially polarized narrow-width annular beam (NWAB) with the double-knife-edge method, they reported that a smallest focal spot with size of $0.0711\lambda^2$ can be obtained with an annular factor of 0.91, and they also pointed out that sharper focus cannot be achieved by an ultra-narrow annular aperture further because the diffraction effect should be considered.

For a long time, an increasing research effort has been put into improving the trapping efficiency [18–24]. It has been shown that the radially polarized beams are superior to the linearly polarized beams in the trapping capability [18–22]. The extremely strong axial component generated by highly focused radially polarized beams provides a large gradient force, whereas it does not contribute to Poynting vector along the optical axis and thus does not create axial scattering and absorption forces. These features are suitable for improving the performance of an optical trap system, especially for trapping metallic particles [18–22]. Considering the difficulty of trapping metallic particles due to their strong scattering and absorption forces, optical trapping of metallic particles has been explored with different types of beams to reduce the scattering and absorption, including cylindrical vector beam [18,19,22]. A double-ring-shaped

*Corresponding authors. Email: qujun70@mail.ahnu.edu.cn (J. Qu); huangwei6@ustc.edu.cn (W. Huang)

radially polarized beam (denoted as R-TEM$_{11}$*) can be used to increase the axial trap distance and to improve the radial trap stiffness for a metallic Rayleigh particle compared to a conventional single-ring-shaped radially polarized beam (denoted as R-TEM$_{01}$*) [22,23]. In this paper, we present an effective method to improve the trapping capability. One can use a radially polarized NWAB, formed by simply blocking the central portion of a radially polarized Bessel–Gaussian beam (BGB, the original doughnut beam), to greatly enhance the radial trap stiffness and broaden the axial trap distance.

2. Highly focused properties of radially polarized annular beams

According to the vector diffraction theory [25], the electric field components in the vicinity of the focus of a radially polarized annular beam can be obtained as follows:

$$\boldsymbol{E}_r(r,z) = \eta \int_{\delta\cdot\alpha}^{\alpha} \cos^{1/2}\theta \sin(2\theta)\ell(\theta)J_1(k_1 r\sin\theta) \times \exp(ik_1 z\cos\theta)d\theta \quad (1)$$

and

$$\boldsymbol{E}_z(r,z) = -2i\eta \int_{\delta\cdot\alpha}^{\alpha} \cos^{1/2}\theta \sin^2\theta\ell(\theta)J_0(k_1 r\sin\theta) \times \exp(ik_1 z\cos\theta)d\theta \quad (2)$$

where the azimuthal component of the electric filed is zero everywhere in the diffraction field. An azimuthally polarized magnetic field can be produced, this field can be found from Maxwell's equations, that is [26],

$$\boldsymbol{H}_\varphi(r,z) = \frac{2\eta n_1}{\mu_0 c} \int_{\delta\cdot\alpha}^{\alpha} \cos^{1/2}\theta \sin\theta J_1(k_1 r\sin\theta) \times \exp(ik_1 z\cos\theta)d\theta \quad (3)$$

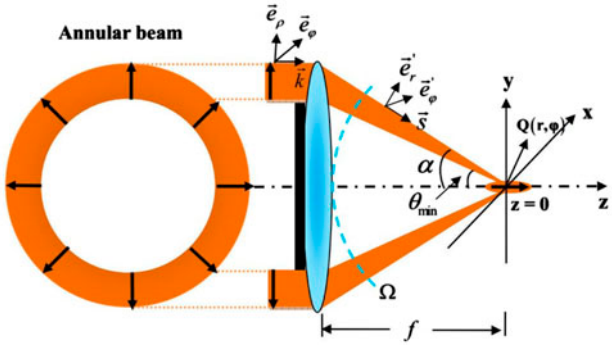

Figure 1. Schematic of a radially polarized NWAB focused by an aplanatic objective lens. The black arrows indicate the direction of the polarization. (The colour version of this figure is included in the online version of the journal.)

In Equations (1)–(3), $\alpha = \arcsin(\mathrm{NA}/n_1)$ is the maximum convergence angle of the objective, and the annular factor δ is defined as the ratio of the inner focusing angle $\theta_{\min}$ to α as shown in Figure 1; $\eta = E_0\pi f n_1/\lambda$ is a constant with f being the focal length, E_0 is the amplitude factor, which is related to the power of the incident beam, $k_1 = kn_1 = 2\pi n_1/\lambda$ is the wave number in the immersion liquid with the refractive index n_1. $J_n(\cdot)$ is the nth order Bessel function of the first kind.

The incident beam is assumed to be a BGB; therefore $l(\theta)$, which represents the amplitude and phase distribution at the exit pupil, can be written as [7,12]

$$\ell(\theta) = \exp\left[-\beta_0^2\left(\frac{\sin\theta}{\sin\alpha}\right)^2\right] J_1\left(2\beta_0\frac{\sin\theta}{\sin\alpha}\right) \quad (4)$$

where β_0 is the ratio of the pupil radius to the beam waist, which is called as the truncation parameter.

The schematic of the focusing of a radially polarized NWAB is shown in Figure 1. A circular blocking mask is placed directly in front of an aplanatic objective lens to generate an annular illumination. We assume the incident beam has a planar wavefront over the pupil, and the aplanatic objective lens can produce a converging spherical wave towards the focus of the lens.

In our calculations, the NA of the focusing lens is set to $0.95n_1$ ($\alpha \approx 71.8°$); the immersion liquid is water with a refractive index of $n_1 = 1.332$, and the laser wavelength (λ) is 1.047 μm, and $\beta_0 = 1.6$. It should be pointed out that when a circular blocking mask is used to form an annular beam, a lot of energy of the incident light beam will be lost. For the sake of comparison, we set the power of the incident beam through the lens which is a constant of 100 mW in our calculations. All the lengths are normalized in units of wavelength. We focus on the influence of the annular factor δ on the focused intensity distribution. Figure 2 shows the intensity distribution of a highly focused radially polarized annular beam in the vicinity of the focus for (a1–3) $\delta = 0$ (the original doughnut beam without a blocking mask) and (b1–3) $\delta = 0.8$ (NWAB), respectively. Comparing the results in Figure 2(a1) and (a2) with that in Figure 2(b1) and (b2), it is seen that a sub-wavelength focal spot (0.32λ) with a quite long depth of focus (about 3λ) can be formed near the focus when a radially polarized narrower annular beam is focused. In contrast to the original doughnut beam, the radial component of the radially polarized NWAB can be largely suppressed while the longitudinal component can be greatly enhanced, as shown in Figure 2(a3) and (b3), making the longitudinal component dominant, thus a smaller focal spot can be expected. The extension of the focal depth can be attributed to the constructive interference between the inner

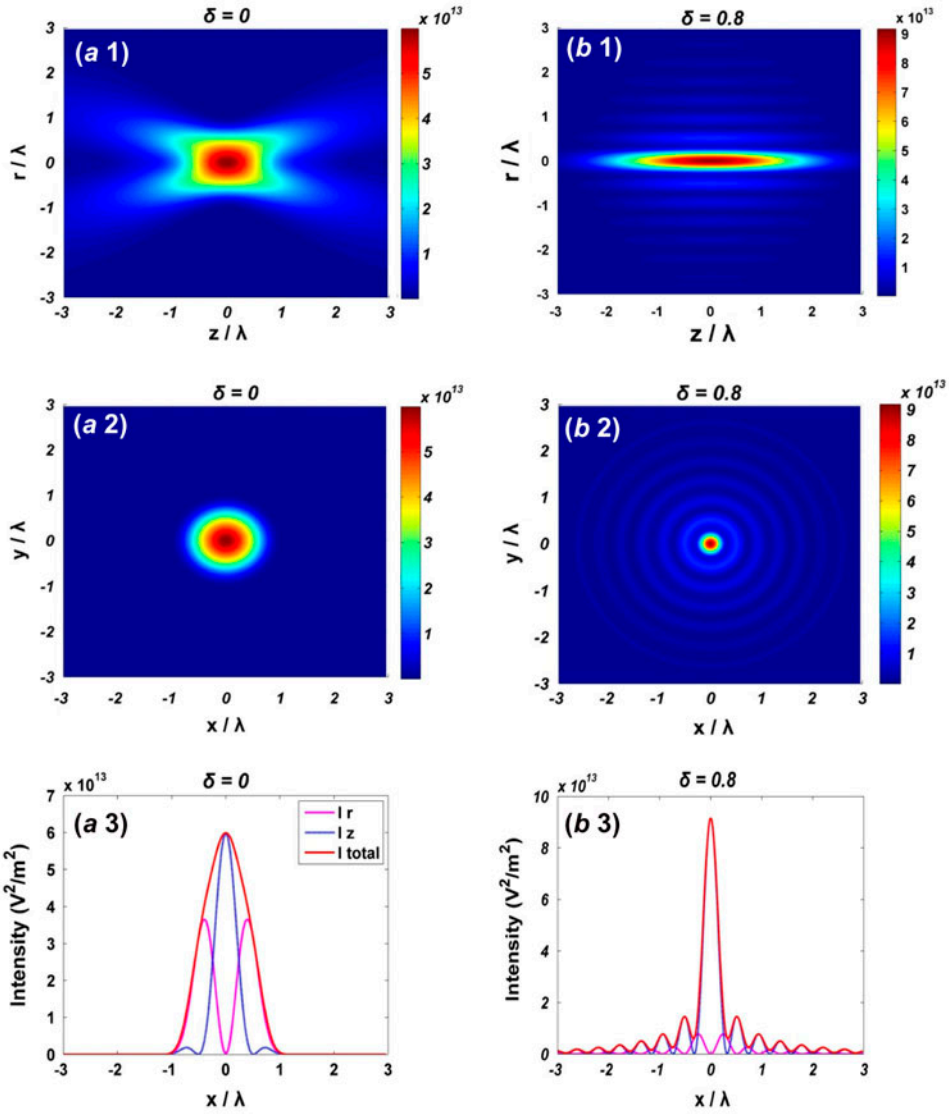

Figure 2. ($a1$) and ($b1$) Contour plots for intensity distribution of radially polarized annular beam in the r–z plane; ($a2$) and ($b2$) Contour plots for the focal spot of radially polarized annular beam in the focal plane; ($a3$) and ($b3$) The cross-section intensity profiles of the radial, longitudinal and the total field components of radially polarized annular beam for $\delta = 0$ and $\delta = 0.8$, respectively. (The colour version of this figure is included in the online version of the journal.)

and outer parts of the annular beam at the focal point. More explicit interpretation can be found in Ref. [7].

We further study the dependence of the focal spot and the depth of focus on the annular factor δ as shown in Figure 3. The depth of the focus is about 1.3λ and the spot size is about 1.05λ in the case of $\delta = 0$, while the depth of the focus extends to about 3λ and the spot size decreases to 0.32λ in the case of $\delta = 0.8$. It is shown that the focal spot size decreases gradually with the increments of δ. For the depth of focus, as the value of δ increases, it will increase slowly at the beginning (about $0 \le \delta < 0.7$), and increase more rapidly with further increasing of δ.

3. Optical trapping forces acting on metallic Rayleigh particles induced by highly focused radially polarized annular beam

As is shown above, a highly focused radially polarized NWAB can generate a sub-wavelength spot size, which is suitable for trapping small particles. Assuming a spherical metallic Reyleigh particle with radius $a (a \ll \lambda)$, such a small particle develops an electric dipole moment in response to the light's electric field. The dipole approximation can be used to calculate the radiation forces [18]. The radiation forces acting on a metallic particle can be divided into three parts: the gradient force $\boldsymbol{F}_g$, the absorption force $\boldsymbol{F}_a$, and the

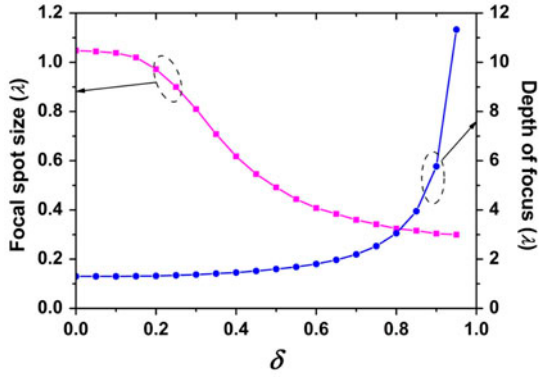

Figure 3. Focal spot size and depth of the focus of radially polarized annular beams as a function of annular factor δ. The other parameters are the same as Figure 2. (The colour version of this figure is included in the online version of the journal.)

scattering force $\boldsymbol{F}_s$. The gradient forces are responsible to pull the particle towards the center of the focus while the scattering and absorption forces tend to destabilize the trap. Thus, stable trapping requires the axial gradient force to dominate. According the Rayleigh scattering theory, these forces can be expressed as [18,21–23]

$$\boldsymbol{F}_g = \mathrm{Re}(\gamma)\varepsilon_0 \nabla |E(r,z)|^2/4 \tag{5}$$

$$\boldsymbol{F}_a = n_1 \langle \mathbf{S} \rangle C_{\mathrm{abs}}/c \tag{6}$$

$$\boldsymbol{F}_s = n_1 \langle \mathbf{S} \rangle C_{\mathrm{scat}}/c \tag{7}$$

where $\gamma = 4\pi a^3 \varepsilon_1(\varepsilon_2 - \varepsilon_1)/(\varepsilon_2 + 2\varepsilon_1)$ is the polarizability of the metallic particle, with ε_2 and ε_1 being the relative permittivity of the particle and the ambient, respectively. $C_{\mathrm{abs}} = kn_1 \mathrm{Im}(\gamma)/\varepsilon_1$ and $C_{\mathrm{scat}} = k^4|\gamma|^2/6\pi$ are the absorption and scattering cross-sections, respectively. The time-averaged Poynting vector of the focused radially polarized annular beam can be expressed as [18,21–23]

$$\langle \mathbf{S} \rangle = [\mathrm{Re}(\boldsymbol{E}_r \boldsymbol{H}_\varphi^*)\hat{\boldsymbol{e}}_z - \mathrm{Re}(\boldsymbol{E}_z \boldsymbol{H}_\varphi^*)\hat{\boldsymbol{e}}_r]/2 \tag{8}$$

In our calculations, we assume that the radius of the gold particle is 19.1 nm, and its relative permittivity is $\varepsilon_2 = -54 + 5.9i$ [18,22]. The other parameters are the same as Figure 2. Figure 4 shows the total transverse trapping force $\boldsymbol{F}_t = (\boldsymbol{F}_{g,t} + \boldsymbol{F}_{a,t} + \boldsymbol{F}_{s,t})$ acting on the gold particle along the x-axis direction for three different values of annular factor δ in the focal plane and at the off-focus distance of $z = \lambda$, respectively. From Figure 4(a), it can be seen that the particle can be trapped at the focus, and the radially polarized narrower annular beam provides a larger total transverse trapping force compared with that of the original beam as expected. It is also found that the origin doughnut beam can't trap the particle at the off-focus distance of $z = \lambda$ anymore, whereas the annular beam can still stably trap the

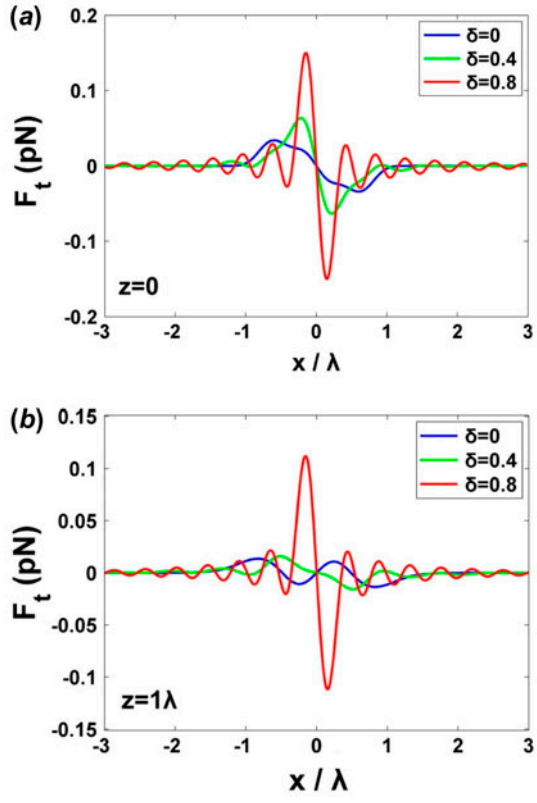

Figure 4. The total transverse trapping force F_t acting on a gold particle along the x-axis for three different values of annular factor for $\delta = 0$, 0.4 and 0.8, (a) in the focal plane, (b) at the off-focus distance of $z = \lambda$, respectively. (The colour version of this figure is included in the online version of the journal.)

particle, as shown in Figure 4(b). We can conclude that one can use a radially polarized NWAB instead of the original doughnut beam to improve the trapping stability and to broaden the axial trap range.

Figure 5 shows the longitudinal gradient force $\boldsymbol{F}_{g,z}$, the sum of the longitudinal absorption and scattering forces $(\boldsymbol{F}_{a,z} + \boldsymbol{F}_{s,z})$, and the total longitudinal trapping force $\boldsymbol{F}_z = (\boldsymbol{F}_{g,z} + \boldsymbol{F}_{a,z} + \boldsymbol{F}_{s,z})$ with three different values of annular factor δ for two cases of on the z-axis and at the *off*-axis distances of $x = 0.15\lambda$, respectively. The calculation parameters are the same as in Figure 4. It is clear from Figure 5(a) that the sum of the scattering and absorption forces is substantially zero along the optical axis due to the vanishing of Poynting flux component under tight focusing conditions, and thus the particle can be trapped longitudinally at the focus. For smaller values of δ, the longitudinal gradient force can be enhanced slightly compared to the usage of the original doughnut beam. For higher values of δ, the longitudinal trap range can be broadened, even though the longitudinal gradient force will be decreased. As shown in Figure 5(b), when the particle locates at an *off*-axis position of $x = 0.15\lambda$, the particle will suffer strong scattering and absorption

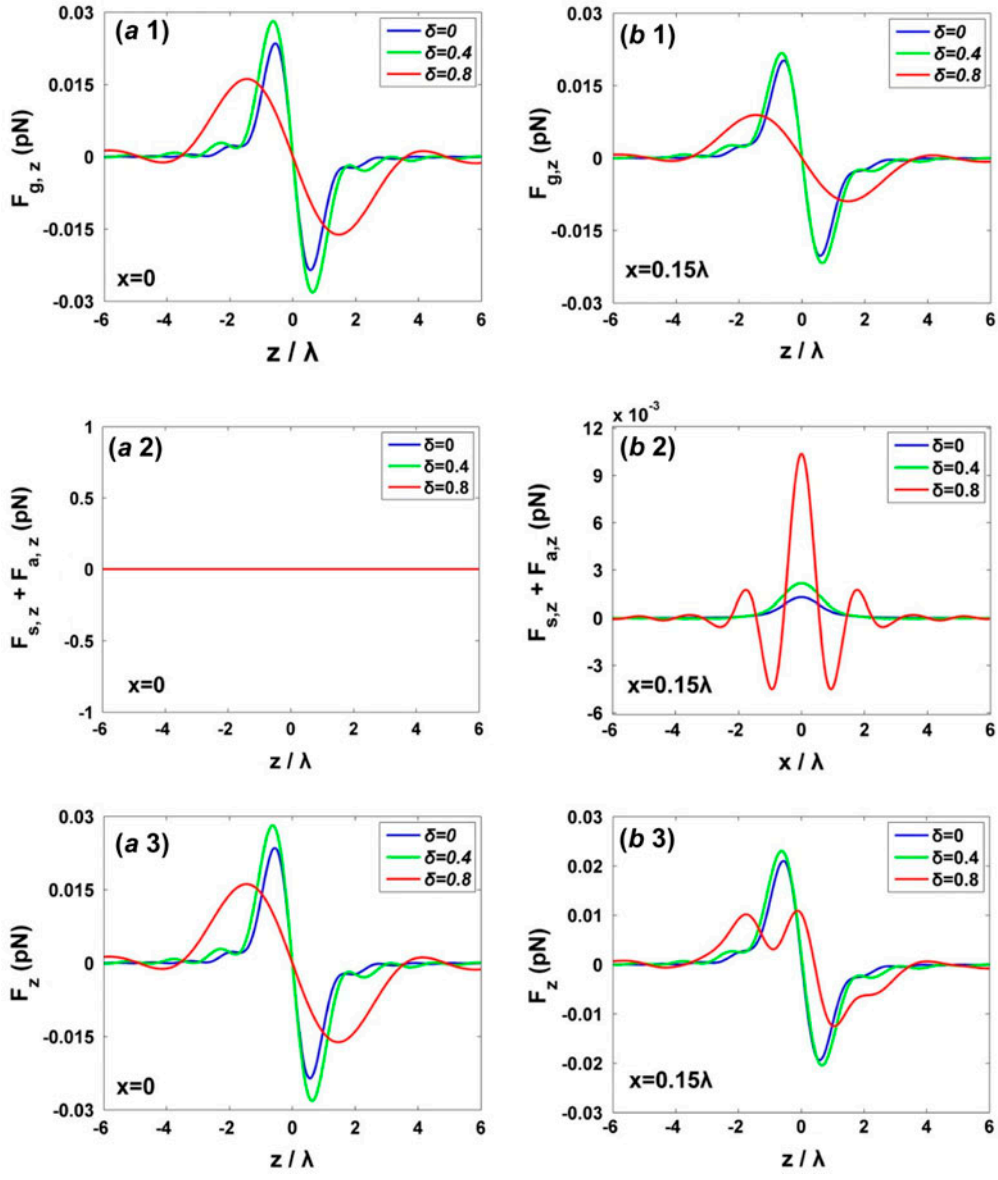

Figure 5. The longitudinal gradient force (top row), the sum of the longitudinal absorption and scattering forces (middle row), and the total longitudinal trapping force (bottom row) for three different values of annular factor for $\delta = 0$, 0.4 and 0.8 at two different off-axis distances of $x = 0$ (left column) and $x = 0.15\lambda$ (right column), respectively. (The colour version of this figure is included in the online version of the journal.)

forces, thus a shift of the trap equilibrium appears along the propagation direction, for example, the trap equilibrium position is $Z_{equ} = 0.406\lambda$ for the case of $\delta = 0.8$.

The transverse and longitudinal trap stiffness can be expressed as [22] $\kappa_t = |\partial \boldsymbol{F}_t/\partial x|X_{equ}$ and $\kappa_z = |\partial \boldsymbol{F}_z/\partial z|Z_{equ}$, respectively. In Figure 6, we plot the dependence of the transverse and longitudinal trap stiffness on the annular factor δ at the focus. It is shown that the transverse trap stiffness increases gradually with the increments of δ, until it reaches its maximum value (approximately at $\delta =$ 0.75), which is more than 10 times larger than that of the original beam. Then the transverse trap stiffness decreases rapidly with further increasing of δ, this peculiar behavior may be attributed to the diffraction effect. It is also found that by increasing the value of δ, the longitudinal trap stiffness has a slight increase at the beginning ($\delta < 0.4$), and then decreases as δ increases further due to the extension of the focal depth. The most feasible method of improving the trap stability is to choose a suitable width of the annular beam by adjusting the radius of the blocking mask.

The small particle always suffers the Brownian motion due to the thermal fluctuation from the surrounding medium. Following the fluctuation-dissipation

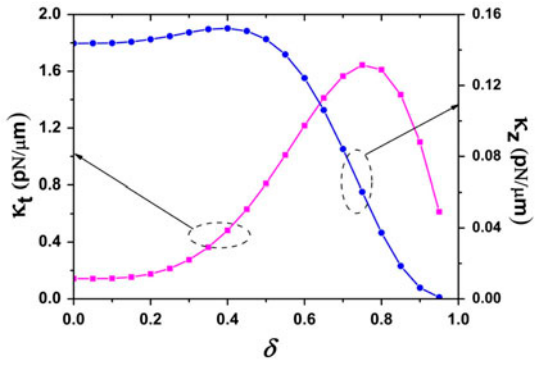

Figure 6. Dependence of the transverse and longitudinal trap stiffness on the annular factor of δ at the focus point, respectively. (The colour version of this figure is included in the online version of the journal.)

theorem of Einstein, the magnitude of the Brownian force is expressed as [27] $|f_B| = (12\pi\kappa a k_B T)^{1/2}$ with κ being the viscosity of the surrounding medium, k_B being the Boltzmann constant, and T being the temperature of the surrounding medium. For the case of $T = 300$ K, the magnitude of the Brownian force is 1.542×10^{-3} pN, which is much smaller than the gradient forces, thus the influence of the Brownian motion can be neglected.

4. Conclusions

In summary, we have theoretically investigated the focusing properties and the optical trapping forces acting on a gold Rayleigh particle produced by a highly focused radially polarized NWAB, formed by subtly blocking the central portion of a radially polarized BGB. For the sake of comparison, the case of the original doughnut beam is also calculated under the same conditions. Our results show that a sub-wavelength spot size with long depth of focus can be generated by focusing a radially polarized NWAB. More importantly, these features are suitable for trapping small particles. One can use a radially polarized narrower annular beam to largely enhance the transverse trapping stability and broaden the longitudinal trap range compared to the usage of the original doughnut beam. Our research presents an innovative method to improve the trapping capability, which will be useful for experimental trapping by means of optical tweezers.

Funding

This work is supported by the National Natural Science Foundation of China (NSFC) under [grant numbers 21133008 and 11374015]. Acknowledgment is also made to the Thousand Youth Talents Plan.

References

[1] Ashkin, A.; Dziedzic, J.M.; Bjorkholm, J.E.; Chu, S. *Opt. Lett.* **1986,** *11*, 288–290.
[2] Chu, S. *Rev. Mod. Phys.* **1998,** *70*, 685–706.
[3] Mitchem, L.; Reid, J.P. *Chem. Soc. Rev.* **2008,** *37*, 756–769.
[4] Dear, R.D.; Burnham, D.R.; Summers, M.; McGloin, D. *Phys. Chem. Chem. Phys.* **2012,** *14*, 15826–15831.
[5] Zhong, M.; Wei, X.; Zhou, J.; Wang, Z.; Li, Y. *Nat. Commun.* **2013,** *4*, 1768.
[6] Grier, D.G. *Nature* **2003,** *424*, 810–816.
[7] Kitamura, K.; Sakai, K.; Noda, S. *Opt. Express* **2010,** *18*, 4518–4525.
[8] Kozawa, Y.; Sato, S. *Opt. Lett.* **2006,** *31*, 820–822.
[9] Tian, B.; Pu, J. *Opt. Lett.* **2011,** *36*, 2014–2016.
[10] Dorn, R.; Quabis, S.; Leuchs, G. *Phys. Rev. Lett.* **2003,** *91*, 233901.
[11] Yang, L.; Xie, X.; Wang, S.; Zhou, J. *Opt. Lett.* **2013,** *38*, 1331–1333.
[12] Wang, H.; Shi, L.; Lukyanchuk, B.; Sheppard, C.; Chong, C. *Nat. Photonics* **2008,** *2*, 501–505.
[13] Hao, X.; Kuang, C.; Wang, T.; Liu, X. *Opt. Lett.* **2010,** *35*, 3928–3930.
[14] Dong, Y.; Wang, F.; Zhao, C.; Cai, Y. *Phys. Rev. A* **2012,** *86*, 013840.
[15] Chen, R.; Dong, Y.; Wang, F.; Cai, Y. *Appl. Phys. B* **2013,** *112*, 247–259.
[16] Zhan, Q. *Adv. Opt. Photon.* **2009,** *1*, 1–57.
[17] Zhang, Y.; Bai, J. *Opt. Express* **2009,** *17*, 3698–3706.
[18] Zhan, Q. *Opt. Express* **2004,** *12*, 3377–3382.
[19] Huang, L.; Guo, H.; Li, J.; Ling, L.; Feng, B.; Li, Z. *Opt. Lett.* **2012,** *37*, 1694–1696.
[20] Kozawa, Y.; Sato, S. *Opt. Express* **2010,** *18*, 10828–10833.
[21] Yan, S.; Yao, B. *Phys. Rev. A* **2007,** *76*, 053836.
[22] Zhang, Y.; Suyama, T.; Ding, B. *Opt. Lett.* **2010,** *35*, 1281–1283.
[23] Zhang, Y.; Ding, B.; Suyama, T. *Phys. Rev. A* **2010,** *81*, 023831.
[24] Gu, M.; Morrish, D.; Ke, P. *Appl. Phys. Lett.* **2000,** *77*, 34–36.
[25] Youngworth, K.S.; Brown, T.G. *Opt. Express* **2000,** *7*, 77–87.
[26] Zhang, Y.; Ding, B. *Opt. Express* **2009,** *17*, 22235–22239.
[27] Okamoto, K.; Kawata, S. *Phys. Rev. Lett.* **1999,** *83*, 4534–4537.